Influence of the Presence of CO_2 in the Feed of an Indirect Heating TSA Process for VOC Removal

M. CLAUSSE, J. BONJOUR AND F. MEUNIER
CNAM-Laboratoire du Froid (E.A. 1408), 292 rue Saint Martin 75003, Paris, France
meunierf@cnam.fr

Abstract. This work deals with an experimental study of an indirect temperature swing adsorption process for VOC removal from air or for gas purification. A 1 m long and 70 mm diameter column with an internal heat exchanger has been filled with Ambersorb 600 carbonaceous adsorbent. This column is equipped with sensors to measure temperature at several points inside the bed, as well as the inlet and outlet gas concentration, pressure, temperature and mass flow. In a first step, CO_2 or ethane/dry nitrogen mixtures were used to simulate a single VOC in air, with different concentrations (350 ppm, 1% and 10%). As a first results very effective gas purification was obtained and an advantage of this process is the high pollutant concentration during the regeneration phase. Experiments were performed with various ethane/CO_2 mixtures. The influence of the presence of CO_2 on the ethane concentration breakthrough curves and on the ethane concentration during regeneration is reported. The IAS theory was used, as a first approach, to predict the adsorbed pollutants amount. Relatively good prediction is obtained with a maximum error in the order of 10%. An energy balance study is reported as well.

1. Introduction

One advantage of TSA (Thermal Swing Adsorption) processes is that it is possible to desorb strongly adsorbed species, which is often difficult using PSA (Pressure Swing Adsorption) processes. However, the disadvantage of TSA processes is that they require large adsorbent inventory. This is due to the fact that the regeneration step is long so that the beds are not used as often as in PSA processes. If one wants to reduce the adsorbent inventory, the solution is to design rapid adsorbers so as to operate more cycles. The challenge is to be able to reduce the regeneration step from about one hour to a few minutes. To go towards that direction, at least three tasks are required:

– to analyze and improve the heat transfer in the heat exchanger, and to optimize the column geometry,
– to choose optimized cycle parameters (cycle times, flow rates, . . .), whose values depend on the feed composition, so as to improve the cycle global efficiency,
– to design a multibed process in order to reach a high working capacity when compared to a single bed process.

Most of studies on TSA cycles use direct steam regeneration (LeVan, 1989) and few studies with indirect heating do exist (Salden et al., 1998; Bonnissel et al., 1998; Burchell et al., 1997). Nevertheless these novel TSA processes mainly use electricity as source power. The objective of the present paper is the study of a new indirect TSA process for the removal of volatile organic components (VOC) from air streams in the presence of CO_2. The first two tasks presented above are undertaken for to this new process in the following. The VOC is simulated by ethane, while dry nitrogen was substituted to air. The goal for studying the co-adsorption of CO_2 with another gas is two-fold:

– CO_2 is present in air and it is important to know its impact on VOC removal

– CO_2 separation and sequestration is one of the possible ways to lower greenhouse effect (Reichle et al., 1999).

However, for CO_2 sequestration to be environmentally self-consistent, the process-induced CO_2 emission must be lower than the amount of captured CO_2. The advantage of this TSA process is that it can be an integrated process using waste heat, which would not at all contribute to greenhouse effect.

Indeed, the originality of the adsorber presented herein comes from the indirect heating during the regeneration step of the process using a rapid HX. Heating is performed in a two-phase heat transfer mode, namely condensation of steam. This allows to reach high heat transfer coefficients, which reduces the regeneration time. As it is well known, in a purification process, the adsorption step is much longer than the regeneration step. It is the reason why several beds are used and, generally, one bed is under regeneration when the other beds are under adsorption. The number of beds to be used depends on the time ratio between the two steps. Moreover, contrarily to direct steam regeneration, an indirect TSA allows to recover the VOC without the presence of water, which, in case of miscible VOC may be important.

2. Description of Experiments

Before running cycles, preliminary experiments are needed in order to collect information on the column performances with the selected pollutant or mixture at different inlet concentrations. So, complete breakthrough or regeneration were performed with various flow rates for each step (typically between 10 and 20 Ndm^3/min total flow rate for the adsorption phase and zero, 0.2 or 2 Ndm^3/min of nitrogen purge for the pre-heating/regeneration step). These experiments allowed to determine the expected pollutant concentration during regeneration, the cycle maximum phase times, etc.

The full cyclic process includes two main steps: adsorption and regeneration. However, a pre-cooling step is necessary before the purification/adsorption and a pre-heating step with reduced purge flow rate was used, as shown on Fig. 1. The pre-heating step with a very small purge flow rate (generally 0.2 Ndm^3/min) is introduced to obtain concentrated pollutant in the exhaust gas. This phase duration is constant for all the cycle experiments presented below ($T_1 = 10$ min). The actual regeneration step with a purge flow rate (generally 2 Ndm^3/min) lasts $T_2 = 20$ min. Besides, as will be seen below, two protocols have been tested: in the first case, the heat is provided during time $T_1 + T_2$, whereas in the second case, the column is heated during time T_1
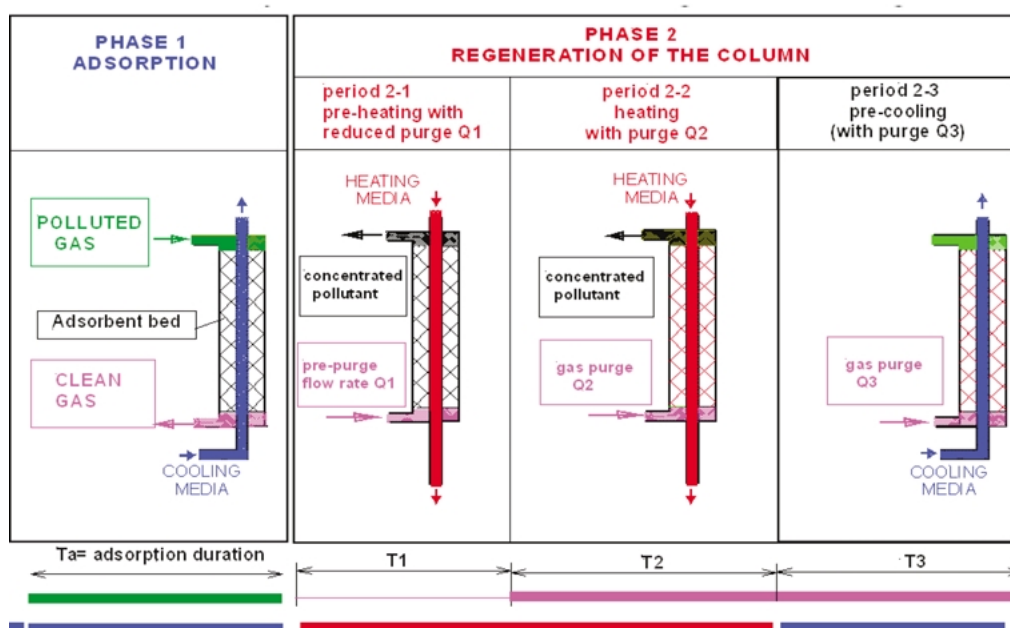

Figure 1. TSA cycle with indirect heating and cooling.

only. If heating is stopped during the regeneration, the desorption is due to the thermal inertia of the bed and to the nitrogen circulation. Once the column is regenerated, the pre-cooling step starts and lasts $T_3 = 10$ min. Lastly, the adsorption step time depends on the species to be adsorbed (and is set from the preliminary experiments) and on the feed concentration.

3.   Experimental Set Up and HX Qualification

3.1.   Geometry and Instrumentation

The adsorber is a 1 m high heat exchanger (HX) with 12 external fins (Fig. 2). It is made of concentric tubes (inner tube outer diameter: 19 mm, outer tube inner diameter: 70 mm), to form an annulus (internal volume: 3.65 dm^3) filled with an adsorbent (mass of adsorbent: 1.96 kg).

Several parameters are measured during the experiments. Thermocouples, with an accuracy of about ± 1 K, are placed at five horizontal cross-sections of the column (referenced P1 to P5 accordingly to the notations on Fig. 2) corresponding to the following distance from the top: $z = 6$ cm, 27.5 cm, 50 cm, 72.5 cm and 95 cm respectively. For cross-sections P1, P3 and

Figure 2. Adsorber geometry and location of the temperature measurements.

P5, thermocouples are placed at five radial and angular locations (referenced A, B, C, D and E accordingly to the notations on Fig. 2). For cross-sections P2 and P4 only two locations are used (C and D).

During the desorption phase, the condensed water is collected in a tank equipped with a level indicator, which allows to measure the steam consumption. A differential manometer is used to measure the pressure drop through the porous bed. The gas mixture composition is determined at the outlet of the column by gas chromatography which detection limit was found to be 50 ppm. The inlet composition is fixed by the ratio of the flow rates of each gas, which is adjusted by mass-flow controllers (uncertainty of 1%).

Although TSA process is recommended for strongly adsorbed species, ethane was chosen for experimental reasons, i.e., avoiding the cycles to be too long, owing to such a moderately adsorbed molecule. The Ambersorb 600 is a carbonaceous adsorbent made of highly sulfonated styrene/divinylbenzene resin. It was selected as adsorbent because of the small size and the spherical shape of the particles (mean diameter of 0.65 mm) to reduce dispersion effects. Furthermore, the hardness of this kind of carbonaceous adsorbent is superior to that of classical activated carbon, which prevents from excessive mechanical attrition.
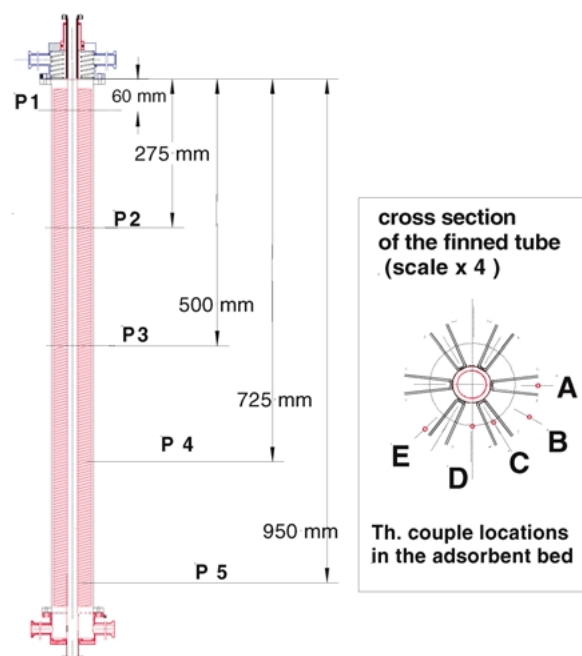
3.2.   Heat Exchanger Qualification

Heating is obtained by means of a downward circulation of condensing steam inside the inner tube. Thanks to the use of condensation in the inner tube during the heating stage, it has been shown previously that very high wall heat transfer coefficients (up to 7000 W/m$^2 \cdot$ K) can be reached on the vapor side, so that the heat transfer limitation is not due to the heating medium (Mativet, 1997; Mativet et al., 1999). As regards the adsorption phase, cooling is realized by circulating upward a volume flow of 400 L/h of cool water (10 to 25°C) inside the inner tube. At the beginning of the cooling period, if the inner tube is at a temperature higher than 100°C, the water is boiling and removes heat from the bed very quickly with a high heat transfer coefficient (about 1000 W/m$^2 \cdot$ K). This lasts as long as the wall superheat is high enough to maintain bubble nucleation but, once this transient boiling period is finished, the heat transfer is due to single-phase convection. The time during which boiling occurs was found to be much shorter (10 to 30 s for a bed initially at 150°C) than the typical adsorption
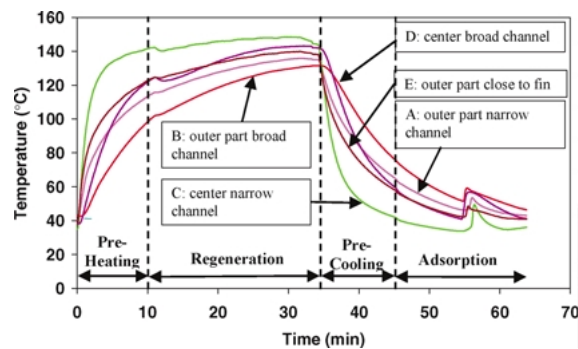
Figure 3. Temperature evolution at the column mid-height during a cycle (ethane feed concentration: 10%—steam temperature: 150°C).

times so that it can be concluded that thanks to the thermal performances of the column, a high temperature at the beginning of adsorption does not drastically limit the adsorption capacity of the bed.

First, a series of experiments were performed to test the heat transfer characteristics of the HX: very small axial temperature gradients are observed (less than 8 K, as shown by Bonjour et al. (2000)). However, much larger radial temperature differences, up to 70 K (from the center of the narrow channels to the outer part of the broad channel), exist (Fig. 3) especially during the pre-heating step. This phenomenon obviously limits the desorption rate in the coolest zones of the column during the pre-heating step. The internal HX concept allows already to run short time cycles (the average bed temperature reaches 90% of the regenerating temperature in 20 min), but the HX geometry could still be improved to achieve shorter time cycles. In addition, Fig. 3 also shows an adsorption-induced thermal wave due to the adsorption front at the bed mid-height.

4.   Single Pollutant Experimental Results

Experiments were performed on the adsorption of pure gases (ethane or CO_2) mixed with nitrogen, which was used to simulate dry air. The values of characteristic times are reported in Table 1 for both components. Breakthrough curves for the adsorption of ethane are shown on Fig. 4 for the same flow rate (20 Ndm^3/min) but with two feed concentrations (1% and 10%). They are plotted under reduced coordinates, i.e., ratio of outlet to feed concentration vs. ratio of time to breakthrough time. It is noticeable that under this reduced form, the breakthrough curves are independent from the feed composition. This remark also stands for the

Table 1. Characteristic times for single pollutant breakthrough non-cyclic experiments ($T_{bed} = 25°C$).

Feed	Breakthrough time (min)	99.995% purity nitrogen recovery (min)
1% C_2H_6—20 Ndm^3/min	96	63
10% C_2H_6—20 Ndm^3/min	34	22
1% CO_2—20 Ndm^3/min	18.5	13
10% CO_2—20 Ndm^3/min	13	8
350 ppm CO_2—20 Ndm^3/min	19.5	12
350 ppm CO_2—10 Ndm^3/min	43	30

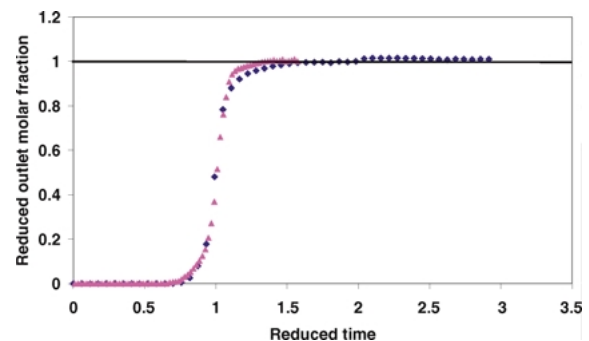*Figure 4*. Ethane reduced breakthrough curves (20 Ndm^3/min total flow rate—$T_{bed} = 25°C$) ◆ 1% ethane, ▲ 10% ethane.

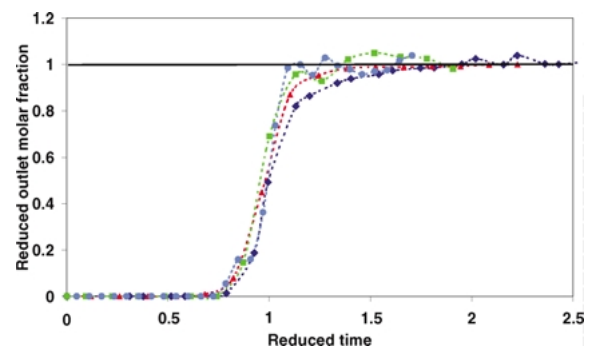*Figure 5*. Reduced CO_2 breakthrough curves at different flow rates and inlet concentrations ($T_{bed} = 25°C$) ◆ 10% CO_2 20 Ndm^3/min, ▲ 1% CO_2 20 Ndm^3/min ■ 350 ppm CO_2 20 Ndm^3/min, ● 350 ppm CO_2 10 Ndm^3/min.

reduced breakthrough curves of CO_2 at different concentrations (350 ppm, 1% and 10%) and for two flow rates (10 Ndm^3/min and 20 Ndm^3/min) that are shown on Fig. 5. All these breakthrough curves are reasonably sharp and no important problems of internal mass transfer resistance do appear. For both pollutants, the nitrogen purity at the column outlet was found to be
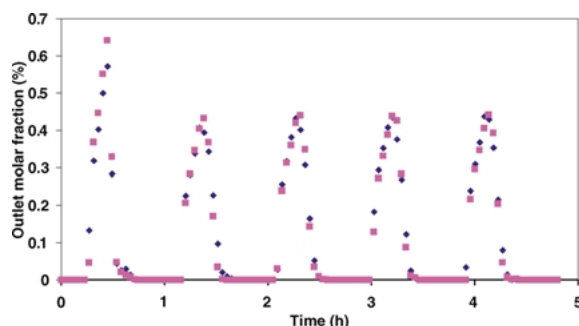
Figure 6. Influence of heating during regeneration on CO_2 outlet concentration (■ Continuous heating, ◆ Heating stopped after pre-heating).

Figure 7. Influence of heating protocol during regeneration on temperature and desorbed mass.

better than 99.995% (chromatograph detection limit) until a reduced time between 0.6 and 0.7 for both CO_2 and ethane.

Figure 6 shows the outlet gas composition during successive cycles (adsorption, regeneration) with a 350 ppm CO_2 feed during adsorption. Two series of cycles are presented. They correspond to the two experimental protocols mentioned previously, i.e., providing heat by condensing steam during the pre-heating step, but heating or not during the regeneration step. It has to be noted that a periodic behavior is reached very rapidly after the second cycle, which is considered as usual in TSA processes (Yang, 1987). In this case, the choice of the protocol has very little effect on the cyclic column behavior. For both protocols, the maximum CO_2 concentration during the desorption reaches 0.4% (4000 ppm) and the average concentration is about 0.28%. Following the definition given by Davis and LeVan (1989), the enrichment ratio (ratio of average recovered pollutant concentration to feed concentration) reaches 8. Similar results, which are not shown here, were obtained with ethane and presented by Bonjour et al. (2002). The enrichment ratios were found to be 4.3 and 18 for a 10% and 1% feed, respectively.

Figure 7 shows the bed mean temperature and cumulative desorbed mass of CO_2 during the regeneration stage of the previously described cycles. If heating is stopped at the end of the pre-heating phase, the bed temperature slightly decreases from its maximum value (125°C) by about 5 K. However, the heating protocol has no effect on the mass of desorbed CO_2. Indeed, the bed thermal inertia is high enough so that the temperature decrease remains limited. Moreover, the CO_2 isotherms at 120 and 125°C are flat and very close the one to the other. Therefore, this protocol (heating during the pre-heating phase only) is better from the
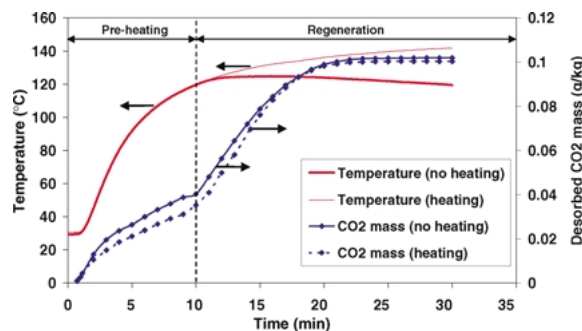
energetic point of view. In both cases, the desorbed mass at the end of the pre-heating step is about 37% of the total desorbed mass. This performance is achieved in about one third of the overall regeneration time. This illustrates that even if radial temperature gradients do exist as shown in Section 3.2, the temperature rise is fast enough to ensure appropriate desorption during this step. From Fig. 7, one can also observe that the cumulated desorbed mass reaches its asymptotic value after 20 to 25 min, which means that the regeneration time for operating cycles could probably be reduced by 5 to 10 min.

5. Pollutant Mixtures Results

Adsorption and regeneration experiments were performed with CO_2—ethane mixtures, with nitrogen as carrier gas. For these experiments, the ethane inlet molar fraction was set to 1% and for CO_2, two inlet molar fractions were tested: 10% and 30%. For simplicity, the initial feeds 10% CO_2–1% C_2H_6 and 30% CO_2–1% C_2H_6 will now be designed by feed#1 and feed#2, respectively.
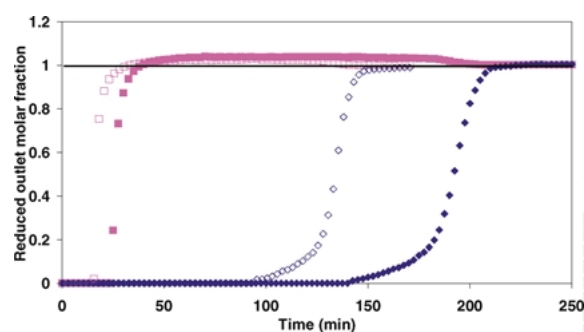
5.1. Breakthrough Experiments

The breakthrough curves, obtained for 10 Ndm³/min total flow rate, are shown in Fig. 8 in terms of reduced outlet molar fraction (ratio of the outlet to the feed molar fraction) as a function of time. The breakthrough time for each component is defined as the time at which the outlet molar fraction equals half of the feed concentration. It is reported for feed#1 and feed#2 in Table 2.

The comparison of the breakthrough times for the mixtures with respect to single components shows that:

Table 2. Breakthrough time and processed mass for different feeds (10 Ndm^3/min–T_{bed} 10°C).

	Inlet molar fraction (%)		Breakthrough time (min)		Processed mass (g)	
	CO_2	C_2H_6	CO_2	C_2H_6	CO_2	C_2H_6
Ethane only	0	1	n.a.	229	n.a.	31
CO_2 only	10	0	33	n.a.	65	n.a.
CO_2 only	30	0	20	n.a.	118	n.a.
Feed#1	10	1	26	192	51	26
Feed#2	30	1	16	134	94	18

Figure 8. CO_2 (□, ■)—C_2H_6 (◇, ◆) breakthrough curves ($T_{bed} =$ 10°C) (black dots for feed#1, white dots for feed#2).

– for feed#1, the breakthrough time of CO_2 and ethane are moderately reduced when compared to single components ones. In terms of capacity (processed mass), the loss is about 20%.
– for feed#2, the breakthrough time of ethane is strongly reduced by the presence of CO_2 (42% loss in terms of capacity) but for the CO_2, the loss is of the same order as for the feed#1.

Therefore, if the goal of the purification process is to recover pure nitrogen, the process will not be much affected by the presence of 1% ethane for these feeds. Nevertheless, in this case the adsorption time will be fairly short (around 10 min for feed#2). This will necessitate a rapid regeneration step to have reasonable working ratios.

On the other side, the process exhibits a very good ability to remove ethane from CO_2. Indeed, production of ethane-free CO_2 is ensured during 130 min for feed#1 and 80 min for feed#2. This pure CO_2 recovery allows an easy post treatment (e.g., sequestration) if the objective is greenhouse gases emission reduction. In enhanced hydrocarbon recovery process, CO_2

under pressure is used to dissolve residual hydrocarbon (Nicholson and Gubbins, 1996). In this case, the column allows to remove hydrocarbons from the CO_2 which will be re-used as solvent.

5.2. Regeneration Experiments

For regeneration experiments, the same operating conditions as for the single component cases were kept (purge nitrogen flow rate at 0.2 Ndm^3/min during pre-heating and 2 Ndm^3/min during regeneration, regenerating temperature at 150°C) in order to easily compare the results. In Figs. 9 and 10, the outlet molar fraction and cumulated desorbed mass curves are plotted as a function of time for feed#1 and #2, respectively.

Very high CO_2 outlet concentrations are achieved during the pre-heating step (up to 70% for feed#1 during adsorption and 90% for feed#2). Concerning ethane, an almost plateau zone is observed during the pre-heating and the main part of the regeneration, the concentration being about 25% for feed#1
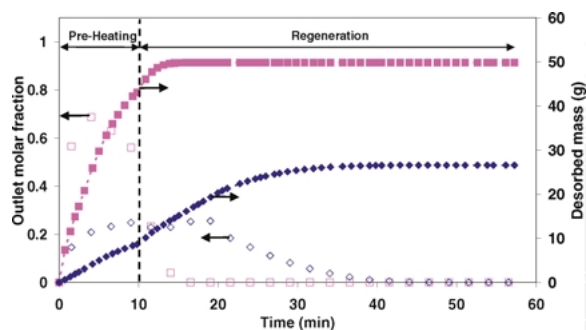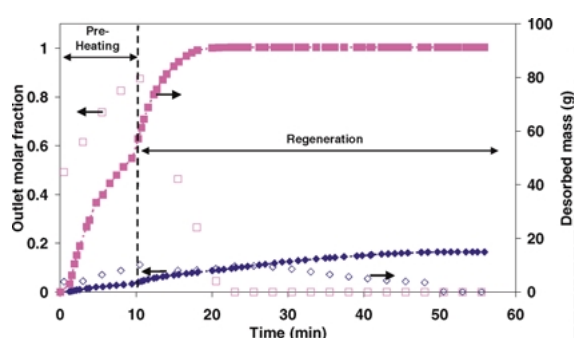

Figure 9. Desorbed mass and concentration curves for 10% CO_2–1% ethane load (CO_2 □, ■, ethane ◇, ◆, black dots for desorbed mass, white dots for concentration).

Table 3.   Desorbed mass values and characteristic times during the regeneration step.

		Overall regeneration step		Pre-heating	
		Total desorbed mass (g)	Time for 90% of recovered mass (min)	Desorbed mass (g)	% of total desorbed mass
Feed#1	CO_2	50	10	45	90
	C_2H_6	27	27	9	33
Feed#2	CO_2	91	13	52	57
	C_2H_6	15	39	3.5	23

Figure 10.   Desorbed mass and concentration curves for 30% CO_2–1% ethane load (CO_2 □, ■, ethane ◇, ◆, black dots for desorbed mass, white dots for concentration).

and 10% for feed#2. Some values of desorbed mass and characteristic time during the regeneration step are reported in Table 3. For feed#1, more than 90% of the CO_2 and 33% of the ethane are desorbed at the end of the pre-heating. For feed#2, only 65% of the CO_2 and 23% of the ethane are desorbed at this time. Furthermore, the time at which 90% of the ethane is desorbed, is 27 min for feed#1 and 39 min for feed#2. CO_2 is seen to be desorbed first which is due to the fact that ethane is more strongly adsorbed. However, the CO_2 load heavily influences the ethane desorption as well as it affects adsorption. For feed#1, CO_2 desorption is achieved in 10 min and ethane desorption lasts about 30 min. For feed#2, more CO_2 is desorbed so that the CO_2 desorption lasts 13 min. For ethane, the desorption lasts longer (about 40 min) for feed#2 than for feed#1, although less ethane has to be desorbed (15 g and 27 g, respectively).

The ratio between the ethane breakthrough stoechiometrics time and the time at which the ethane concentration is equal to the ethane feed concentration is 4.8 for feed#1 and 2.7 for feed#2. These results highlight the regeneration time reduction thanks to the HX

which will allow to design TSA processes with reduced adsorbent inventory (Ruthven, 1984).

5.3.   Comparison with IAS Isotherms

To describe the co-adsorption of ethane and CO_2 on this adsorbent, the IAS theory is chosen as a first approach. The studied mixture is a ternary one with two absorbable species (ethane and carbon dioxide) and one inert (nitrogen). So, the mixture behaves like a binary one for the adsorption phenomenon but the nitrogen mole fraction has to be taken into account for the gas phase. As for all the mixture feeds studied in the experimental section the ethane mole fraction was 1%, this value is chosen for ethane for the IAS isotherm determination. In consequence, the carbon dioxide molar fraction ranges from 0 to 99%, and the nitrogen one is the difference between 100 and the two pollutants mole fractions. The IAS isotherms are plotted on Fig. 11 at atmospheric pressure and for four temperatures (10, 20, 50 et 150°C), 10°C being the cooling medium temperature during the adsorption step and 150°C
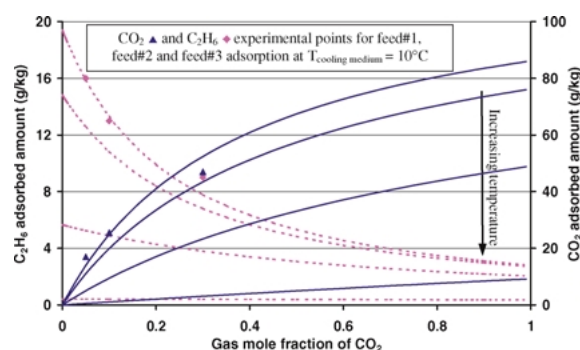

Figure 11. CO_2 (full lines) and ethane (dotted lines) IAS co-adsorption isotherms for four temperatures (10, 20, 50 and 150°C) at atmospheric pressure and for 1% ethane gas mole fraction.

Table 4. Comparison between IAS calculated and experimental adsorbed amounts ($T_{bed} = 10°C$).

	Inlet molar fraction (%)		Experimental (g)		IAS (g)		Error (%)	
	CO_2	C_2H_6	CO_2	C_2H_6	CO_2	C_2H_6	CO_2	C_2H_6
Feed#1	10	1	51	26	50	27	2	4
Feed#2	30	1	94	18	104	16	11	11
Feed#3	5	1	33	32	28	32	15	0

being the heating medium temperature during the regeneration.

The IAS adsorbed amounts and their comparison with the amounts obtained during breakthrough experiments at a temperature of 10°C, for feed#1 (10% CO_2 and 1% C_2H_6), feed#2 (30% CO_2 and 1% C_2H_6) and feed#3 (5% CO_2 and 1% C_2H_6) are reported in Table 4 and in Fig. 11. A very good match is obtained for feed#1. For feed#2 and feed#3 the prediction is less accurate with a maximum error of 15% for the CO_2 amount for feed#3. Nevertheless, it should be remembered that the experimental results are obtained from breakthrough experiments in a column, where pressure and temperature inhomogeneities exist. In consequence, this results in an inhomogeneity of the adsorbed amount in the bed. Nevertheless, the IAS theory gives results accurate enough to be used as a predictive tool for the determination of adsorption time in cycle experiments.

6.   Energy Balance

The consumed energy corresponds to the heat supplied to the bed during the pre-heating and the regeneration steps. It represents almost the only energy needed to run the process as only low energy consuming elements are needed (like a pump for the cooling medium) in contrast with other TSA processes (like a vacuum pump for a VTSA for example).

The second protocol used with CO_2, which consists in reducing the heating time during the regeneration, is very effective with respect to energy consumption since it reduces the heat input by about 25% (from 700 kJ to 525 kJ). However, the use of this protocol can not be generalized. Indeed, if the desorption time is long, without regeneration step heating will lead to unacceptable temperature drop resulting in an increase of the regeneration time.

For the mixtures experiments a complete study was performed. The consumed energy is 1013 kJ for feed#1

and 1044 kJ for feed#2. The corresponding desorption energies are about 93 kJ and 128 kJ. Heat balance on the adsorber allows to evaluate the energy consumption for the whole process. For feed#1 experiments, 29% of the input corresponds to the heat losses, 19% to the adsorbent heating, 23% to the internal HX, 20% to the external tube and about 9.2% to the latent heat of desorption. Similar results are obtained for feed#2 with a latent heat of desorption of about 12%. These results are similar to those presented for ethane by Bonjour et al. (2002). Indeed, the heat is mostly used for as sensible heat for the adsorbent and the HX and the heat losses are about 25–30%. However, the ratios of latent heat (9% for feed#1 and 12% for feed#2) are notably better than for 1% ethane (5% of latent heat) due to greater adsorbed amounts. This highlights that the process performances could be noticeably increased if a multibed configuration was designed. Indeed, the use of a guard bed would allow to reach a small LUB (Length of Unused Bed). In that case, the bed would be almost saturated, so the adsorbed amounts would be maximized, which would result in a better use of the energy.

7.   Conclusions

The aim of this paper was to present the main features of an indirect heating TSA process for the removal of CO_2-ethane mixtures from air. The internal heat exchanger of this process is effective as regards the internal heat transfer (small axial temperature gradients). This allows to quickly warm up the column over its whole length. However, radial temperature gradients are still large. So, improvements on the HX design are needed with four objectives: reducing desorption time, radial temperature gradients, inert mass and heat losses. Work is in progress in this direction (Bejan et al., 2002). However, this process has the main advantage to use low cost energy (waste heat), when compared to other indirect TSA processes (Joule effect, microwaves, etc.) which use electricity.

The breakthrough and regeneration experiments with CO_2—C_2H_6 mixtures allowed to point out the influence of CO_2 inlet concentration on the column performances during both adsorption and regeneration steps. At the concentrations tested, the CO_2 presence reduces the column capacity to capture ethane during adsorption (by 42% for a 30% CO_2–1% C_2H_6 feed when compared to a 1% C_2H_6 feed without CO_2). During the regeneration, the presence of CO_2 increases the necessary regeneration time to completely desorb the column. Even though CO_2 concentration is limiting the process ability to capture ethane, this indirect TSA process showed very good ability to separate CO_2 and ethane, and also to achieve high CO_2 concentration during regeneration.

Furthermore, the column application, i.e., pure nitrogen retrieving or VOC removal and/or CO_2 sequestration, etc., will determine the design of the multi-bed process (column number, serial/parallel arrangement, etc.). Numerical simulation is currently under progress to study such processes.

Acknowledgments

References

Bonjour, J., L.A.O. Rocha, A. Bejan, and F. Meunier, "Dendritic Fins Optimization for a Coaxial Two Stream Heat Exchanger," submitted in *Int. J. Heat Mass Transfer* (2002).

Bonjour, J., A. Mativet, J.B. Chalfen, and F. Meunier, "Identification du coefficient de transfert de chaleur par convection à travers un milieu poreux," *3èmes Journées Tunisiennes sur les Ecoulements et les Transferts, Mahdia (Tunisia)*, 167–171 (2000).

Bonjour, J., J.B. Chalfen, and F. Meunier, "Temperature Swing Adsorption Process with Indirect Cooling and Heating, "*Ind. Eng. Chem. Res.*, **41**, 5802–5811 (2002).

Bonnissel, M., L. Luo, and D. Tondeur, "Fast Thermal Swing Adsorption Using Thermoelectric Devices and New Adsorbent," in *Proc. 6th Conf. Fundamentals of Adsorption (FOA6)*, F. Meunier (Ed.), pp. 1065–1070, Elsevier, 1998.

Burchell, T.D., R.R. Judskins, M.R. Rogers, and A.M. Williams, "A Novel Process and Material for the Separation of Carbon Dioxide and Hydrogen Sulfide Gas Mixtures," *Carbon*, **35**(9), 1279–1294 (1997).

Davis, M.M. and M.D. LeVan, "Experiments on Optimization of Thermal Swing Adsorption," *Ind. Eng. Chem. Res.*, **28**, 778–785 (1989).

LeVan, M.D., "Thermal Swing Adsorption: Regeneration, Cyclic Behavior and Optimization," in *Proc. Adsorption Science and Technology, NATO Advanced Study Institute*, A.E. Rodrigues et al. (Eds.), pp. 339–355, Kluwer, 1989.

Mativet, A., "Étude expérimentale d'un procédé de chauffage et de refroidissement par changement de phase du fluide caloporteur," *Thèse de Doctorat*, Univ. Paris XI (1997).

Mativet, A., F. Meunier, J.B. Chalfen, and C. Marvillet, "Experimental Study of Heat Transfer During Film Condensation in Transient Conditions in a Vertical Smooth Tube," *Exp. Heat Transfer*, **12**, 247–263 (1999).

Nicholson, D. and K.E. Gubbins, "Separation of Carbon Dioxide-Methane Mixtures by Adsorption: Effects of Geometry and Energetics on Selectivity," *J. Chem. Phys.*, **104**(20), 8126–8134 (1996).

Reichle, D., J. Houghton, B. Kane, and J. Ekmann, "Carbon Sequestration Research and Development," *US Department of Energy Report* (1999).

Ruthven, D.M., *Principles of Adsorption and Adsorption Processes*, John Wiley & Sons, 1984.

Salden, A., T. Boger, and G. Eigenberger, "Combined Vacuum and Temperature Swing Adsorption Process for the Removal and Recovery of Organic Components from Waste-Air Systems," in *Proc. 6th Conf. Fundamentals of Adsorption (FOA6)*, F. Meunier (Ed.), pp. 915–920, Elsevier, 1998.

Yang, R.T., *Gas Separation by Adsorption Processes*, Imperial College Press, River Edge, N.J., 1997.